

UAV-assisted Visual SLAM Generating Reconstructed 3D Scene Graphs in GPS-denied Environments

Ahmed Radwan¹, Ali Tourani¹, Hriday Bavle¹, Holger Voos¹, and Jose Luis Sanchez-Lopez¹

Abstract—Aerial robots play a vital role in various applications where the situational awareness of the robots concerning the environment is a fundamental demand. As one such use case, drones in GPS-denied environments require equipping with different sensors (*e.g.*, vision sensors) that provide reliable sensing results while performing pose estimation and localization. In this paper, reconstructing the maps of indoor environments alongside generating 3D scene graphs for a high-level representation using a camera mounted on a drone is targeted. Accordingly, an aerial robot equipped with a companion computer and an RGB-D camera was built and employed to be appropriately integrated with a Visual Simultaneous Localization and Mapping (VSLAM) framework proposed by the authors. To enhance the situational awareness of the robot while reconstructing maps, various structural elements, including doors and walls, were labeled with printed fiducial markers, and a dictionary of the topological relations among them was fed to the system. The VSLAM system detects markers and reconstructs the map of the indoor areas, enriched with higher-level semantic entities, including corridors and rooms. Another achievement is generating multi-layered vision-based situational graphs containing enhanced hierarchical representations of the indoor environment. In this regard, integrating VSLAM into the employed drone is the primary target of this paper to provide an end-to-end robot application for GPS-denied environments. To show the practicality of the system, various real-world condition experiments have been conducted in indoor scenarios with dissimilar structural layouts. Evaluations show the proposed drone application can perform adequately w.r.t. the ground-truth data and its baseline.

I. INTRODUCTION

Employing Unmanned Aerial Vehicles (UAVs), or simply drones, for a wide range of applications, such as monitoring, logistics, surveillance, remote sensing, data acquisition, and disaster management, has attracted the attention of researchers in recent decades [1]–[4]. These robots are equipped with various sensors, including Global Positioning System (GPS), Inertial Measurement Unit (IMU), and vision sensors, aiding them in navigation, accurate localization, path planning, obstacle avoidance, *etc.* [5] However, for indoor

¹Authors are with the Automation and Robotics Research Group, Interdisciplinary Centre for Security, Reliability, and Trust (SnT), University of Luxembourg, Luxembourg. Holger Voos is also associated with the Faculty of Science, Technology, and Medicine, University of Luxembourg, Luxembourg. ahmed.radwan.001@student.uni.lu, ali.tourani, hriday.bavle, holger.voos, jose-luis.sanchezlopez@uni.lu

*This work was partially funded by the Institute of Advanced Studies (IAS) of the University of Luxembourg (project TRANSCEND) and the Fonds National de la Recherche of Luxembourg (FNR) (project C22/IS/17387634/DEUS)

*For the purpose of Open Access, and in fulfilling the obligations arising from the grant agreement, the author has applied a Creative Commons Attribution 4.0 International (CC BY 4.0) license to any Author Accepted Manuscript version arising from this submission.

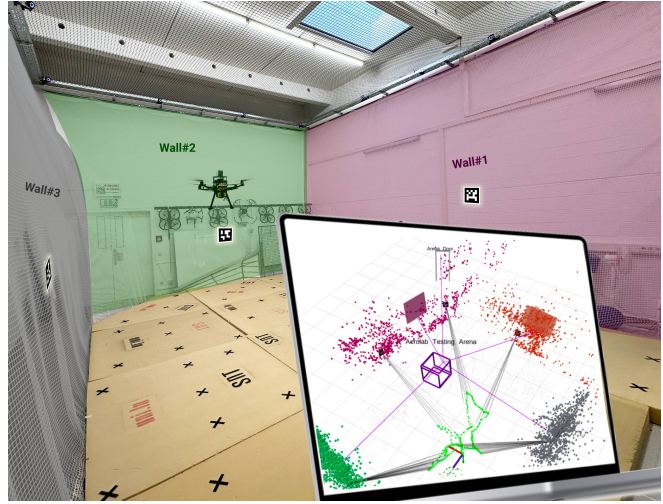


Fig. 1: Reconstructing the map of an indoor environment, along with its 3D hierarchical representation and detected semantic entities generated by integrating a marker-based Visual SLAM framework [8] on a drone.

flights where the GPS signals are missing, relying on other sensors, such as vision sensors (*i.e.*, cameras), is essential for the proper functioning of drones while performing pose estimation and localization [6]. Such sensors aid drones in performing various robotics tasks, including autonomous navigation and Simultaneous Localization and Mapping (SLAM), and improve the robots' Situational Awareness [7].

In this regard, some approaches generate meaningful 3D scene graphs of the environments [9], [10] or incorporate SLAM graphs with 3D scene graphs for richer generated maps representation [11], [12] using Light Detection And Ranging (LiDAR) sensors. However, employing cameras for doing SLAM and using the visual data provided by them for map reconstruction has resulted in the emergence of a new branch known as Visual SLAM (VSLAM) [13]. VSLAM has become more trendy due to incorporating rich visual information for tracking, localization, and mapping steps, along with better scene understanding and semantic object recognition. Particularly, when integrating semantic information and object-based topological relation is targeted, utilizing vision sensors is considered a more attractive approach compared to Light Detection And Ranging (LiDAR)-based solutions [14].

When dealing with cameras as the primary sources of information for VSLAM, there are some challenges in detecting and tracking visual features in the scene. For

instance, facing smooth and feature-less objects such as plaster walls and shiny ceramic tiled floors causes VSLAM system to fail to track and lose localizing data. One of the possible solutions to overcome the mentioned challenges is to employ fiducial markers as artificial landmarks placed on the environment to augment more data for robots [15]. We can see that various fiducial marker libraries, such as ArUco [16] or AprilTag [17], have been used in multiple marker-based VSLAM methodologies, including UcoSLAM [18], sSLAM [19], and TagSLAM [20].

This paper introduces an end-to-end aerial robotics application empowered by a marker-based VSLAM framework (presented by the authors of the paper in [8]) and integrating it into a UAV equipped with a mounted RGB-D camera. The aim is to employ a drone flying in GPS-denied environments to generate tightly coupled visual situational graphs of the areas, along with their low- and high-level semantic entities presented in 3D hierarchies. Accordingly, the primary contributions of the paper in hand are summarized below:

- Preparing a UAV platform equipped with proper sensors and modules for semi-autonomous flight in GPS-denied environments,
- Integration of a VSLAM framework into the mentioned UAV for real-time reconstruction of the maps of indoor areas, enriched with semantic and construction-level objects,
- Wrapping the UAV and the VSLAM framework into an end-to-end situationally aware robot,
- And performing real-world scenario experimental validations using the mentioned system.

II. RELATED WORKS

This section contains state-of-the-art works related to the current research topics, covering the operation of UAVs for indoor environment map reconstruction and generating graph-based 3D representations. Accordingly, studied research works are classified into three categories, listed below:

A. Drone-Assisted Localization and Mapping

Localization of drones and mapping the environments with their particular detected objects has many use cases targeted by drones. In this regard, Raja *et al.* [21] introduced a Particle Filter-based indoor navigation and mapping framework for UAVs that targets precision enhancement for localization and velocity estimation for collision avoidance. In [22], authors introduced a SLAM system for 3D models of environments using photogrammetric and situation mapping with Geographic Information Systems (GIS). In another application, Bhatnagar *et al.* [23] introduced a deep learning-based approach for segmenting images captured by drones to map key vegetation communities. Authors in [24] introduced an indoor localization and tracking methodology based on Acoustic Inertial Measurement (AIM). They use an improved Kalman filter algorithm to reduce location estimation errors and solve tracking challenges in GPS-denied environments. As another research, PILOT [25] is a framework introduced for precise indoor localization in autonomous drones based

on the relative geometrical analysis among transmitters and receivers of ultrasonic acoustic signals. Similarly, ROLATIN [26] is another localization and tracking framework designed for indoor navigation using drones that rely on speaker-generated ultrasonic acoustic signals.

It can be seen that various sensor-based approaches to perform localization, tracking, and mapping exist, which highlights the versatility of the UAVs in addressing related issues. Thus, with advancements in sensor technologies and sensor-fusion approaches, drones are considered potential solutions to be integrated with applications to create accurate maps.

B. VSLAM and 3D Scene Graphs

3D scene graph techniques such as [27]–[29] can generate high-level and optimizable hierarchical representations of environments and depict their recognized semantic entities with suitable relations among them. However, unless other standalone frameworks, such as *S-Graphs* [11], *S-Graphs+* [12] and Hydra [10], where the SLAM maps and scene graphs are tightly coupled, many methodologies target only graph optimization. Considering the introduced advantages of vision sensors, VSLAM methodologies have evolved and become more mature and reliable in recent years. To avoid repetition and save space in the current paper, the authors would like to refer to a survey conducted by them in [30], which provides insights into state-of-the-art approaches in VSLAM, as well as its current trends and potential future directions. Accordingly, reliable and versatile frameworks, such as various versions of ORB-SLAM [31]–[33], have become the baseline for many SLAM approaches that take advantage of vision sensors. Although the geometric maps reconstructed by many methodologies are accurate, fetching semantic entities and adding them to the map can bring about more comprehensible maps and lead to improved optimization outcomes due to considering object-level data associations, as shown in works like [14], [34]–[36].

In this regard, a deep learning-based VSLAM framework that fetches semantic information from the scene to perform multi-object tracking is presented in [37], which augments semantic objects in the reconstructed map. The primary challenge faced with the mentioned methodology is the potential for misclassification of the detected objects. Guan *et al.* [38] proposed a real-time semantic VSLAM methodology, which adds point-object and object-object associations based on the scene segmentation output, in addition to the existing point-point association in ORB-SLAM2. DS-SLAM [39] is another framework that utilizes SegNet for semantic information gathering and semantic mapping. The mentioned approach can work in high-dynamic environments if appropriate processing hardware is provided. Authors in [40] proposed another framework that emerged with a dynamic object removal module for generating static semantic maps. Regardless of the ability of the mentioned methods to map various semantic elements in the environment, many of them may still face challenges due to misidentification and elements' pose estimation errors. In this regard, adding

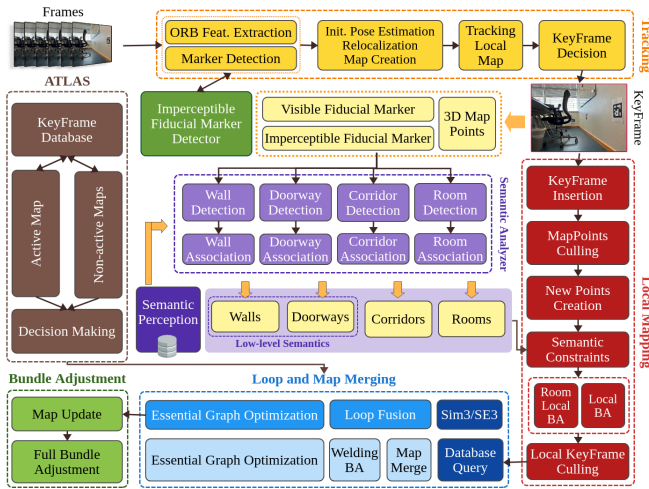


Fig. 2: The primary system components and pipeline of the VSLAM framework used in this research [8].

structural and topological constraints among the detected semantic elements can lead to improved scene understanding, more accurate mapping, and further map optimization.

C. Marker-based VSLAM

As fiducial markers are considered robust tools for augmenting semantic information, several marker-based VSLAM frameworks have been developed for enhanced scene understanding and mapping. Among this, UcoSLAM [18] can perform VSLAM tasks by employing the visual features obtained from both natural and artificial landmarks (*i.e.*, ArUco markers). It contains a marker-based loop closure detector and supports keypoint-only, marker-only, and mixed modes. sSLAM [19] introduced by Romero-Ramirez *et al.* is another similar approach that employs customized markers for robust tracking. The primary contribution of sSLAM is guaranteeing a substantial reduction in resource consumption and computation time while maintaining tracking accuracy. TagSLAM [20] is another methodology that works in marker-only mode and requires having AprilTags in the scene for localization and tracking.

The identifiable gap in the mentioned approaches is reconstructing geometric maps with the aid of fiducial markers while ignoring their potential to augment semantic information. Accordingly, a semantic version of UcoSLAM proposed in [41] can simultaneously generate 3D scene graphs while performing SLAM. It can detect construction-level semantic entities using ArUco markers and utilize their topological relations for optimization. In a similar work, the authors of this paper introduced another marker-based semantic VSLAM framework [8] that provides more accurate reconstructed maps and generates three-layered optimizable hierarchical graphs. Thus, due to the mentioned methodology's advantages and supporting robotics interface for feasible integration, it has been employed in the current paper for an end-to-end drone-based VSLAM system.

III. PROPOSED APPROACH

This section discusses the hardware and software components this paper utilizes for the integration procedure of a VSLAM framework into a drone.

A. Visual SLAM Framework

The framework selected for this work [8] provides more comprehensive reconstructed maps along with their multi-level topological graphs and semantic information derived from fiducial markers. It has been built upon ORB-SLAM3 [33] and adds the required modules to detect ArUco markers, estimate the pose of the semantic objects labeled with the markers, and perform mapping and optimizing based on them. The mentioned approach leverages the ArUco markers affixed to construction-level semantic entities, including walls and doors, reconstructs the semantic map with higher-level semantic entities, including rooms and corridors, and provides hierarchical representations. It should be noted that mapping the high-level semantic entities requires detecting structure-level objects with the help of fiducial markers, along with a database of abstract semantic information about the topological affiliations of the walls and doors labeled with markers.

Fig. 2 depicts the constituent system components and the procedure flow in the mentioned VSLAM system. Accordingly, the framework employs a multi-thread architecture for processing data, including *tracking*, *local mapping*, *loop and map merging*, *bundle adjustment*, and *semantic analysis*. The input visual data provided by an RGB-D camera passes to the fiducial marker detection library and the *tracking* module for extracting ORB features and generating KeyFrame candidates with pose information and 3D map points in the camera and global reference frames. The *local mapping* thread refines the map based on the newly added KeyFrames, markers, and 3D points and triggers the *semantic analysis* module to identify the type of the detected structure-level objects and map them. It should be mentioned that the fetched semantic information also indirectly improves the *local mapping* and *KeyFrame culling* modules. Finally, as the system is constantly cooperating with *Atlas* map manager, *loop and map merging* is handled within active/inactive maps, and local/global *bundle adjustments* is triggered regarding the optimization needed for the reconstructed map.

As the mentioned framework supports Robot Operating System (ROS), integrating it into an aerial robot requires fine-tuning the parameters and configurations and providing proper *topics* to feed camera data.

B. Robot Integration and Adaptation

The aerial robot setup provided in this work for integration with the VSLAM framework and conducting evaluations are shown in Fig. 3. Accordingly, the drone is a *Mikrokopter2* quadrotor built upon the Holybro S500 Quadcopter frame kit with carbon fiber landing gear. It has four Air Gear 450 Combo 2216 Kv880 motors, a LiPo 8000 lite 4S battery pack with 118.4 Wh, and a Flysky controller offering three flight modes (*i.e.*, alt. hold, manual, and Land). The Pixhawk

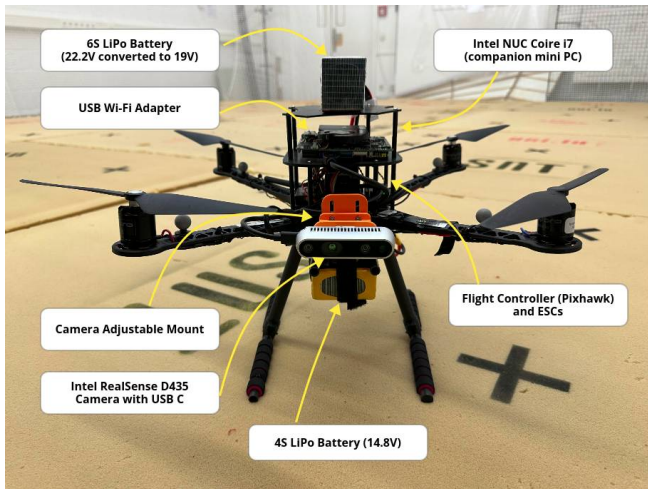


Fig. 3: The drone used in the research for integration with the VSLAM framework and experiments.

4 flight controller of the drone is used to acquire IMU measurements at the rate of 1 kHz adapted to its motor controllers. The vision sensor mounted on the drone is an Intel® RealSense™ Depth Camera D435, providing $87^\circ \times 58^\circ$ Field of View (FoV) and global shutter frame acquisition. An Intel® NUC Kit NUC5i7RYH without housing is mounted onboard as a companion computer, and a desktop computer is used as the Ground Control Station (GCS) for mission commanding and output visualization. The drone has a payload of 1 kg, which carries the 6S battery ($\sim 590\text{g}$), the mini PC ($\sim 220\text{g}$), and the camera ($\sim 75\text{g}$), a total of $\sim 885\text{g}$ of payload. Accordingly, the takeoff of the drone requires $\sim 85\%$ battery throttling.

The firmware programming of the drone contained flashing PX4 and uploading to the Pixhawk, configuring the frame type, flight-related parameters fine-tuning, calibrating the sensors, and setting up the communication protocols. The companion computer was equipped with a ROS Noetic and the required libraries and frameworks for running the system and communicating with the GCS. With the mentioned setup, the VSLAM framework can feasibly work on the drone in both live (online) and offline modes. It should be added that the camera calibration parameters and the dimensions of the fiducial markers are fetched for accurate 3D pose estimation w.r.t. the camera frame.

As can be seen in Fig. 4, there are various conversions for determining the transformations in the system among the robot, camera, marker, and world reference frames. Accordingly, robot-to-world (p_R^G) transformation is done using $p_R^G = T_R^G \cdot p_R$, where T_R^G is the transformation matrix between the robot and the world and p_R is the coordinates of a point in the world reference frame. Similarly, camera-to-robot (p_C^R) transformation is calculated using $p_C^R = T_C^R \cdot p_C$ for the transformation matrix between the camera and the robot T_C^R and the point in the camera reference frame p_C . For marker-to-camera (p_M^C) and marker-to-world (p_M^G) transformations, $p_M^C = T_M^C \cdot p_M$ and $p_M^G = T_M^G \cdot p_M$ are calculated, where

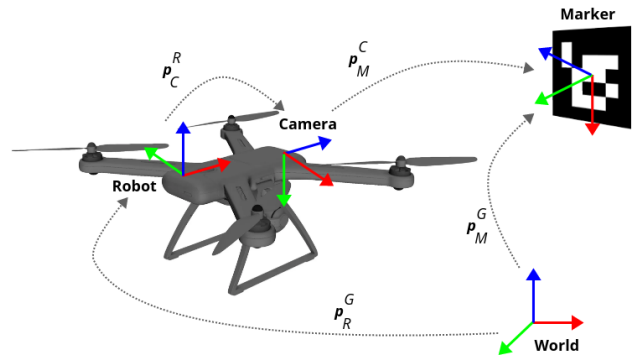


Fig. 4: The reference frames considered in the current framework for perception calculations.

T_M^C and T_M^G the transformation matrix between "the marker and the camera" and "the marker and the world," and p_M is the coordinates of a point in the marker reference frame.

These calculations can aid in coordinating among different reference frames using matrix multiplication and Quaternion operations. It should be added that in the world reference frame, the center is located on the ground with a vertical z -axis. In contrast, in the marker reference frame, the normal vector of the ArUco marker is parallel to the z -axis with a downward x -axis. The robot and camera reference frames are rigidly attached to the UAV and the mounted visual sensor with z -axis values perpendicular to the body and the acquired image plane, respectively.

IV. EVALUATION

This section discusses the evaluation setup and experimental results obtained by employing the designed system. It should be emphasized that the experiments are not conducted to evaluate the performance of the employed VSLAM methodology but instead showcase its functionality and capability in real-world indoor scenarios as an end-to-end situationally-aware UAV system.

A. Evaluation Setup

To evaluate the proposed UAV-assisted VSLAM system in real-world scenarios, the robot introduced in Section III-B was employed. For collecting data, the walls and door frames of various indoor environments with dissimilar configurations and layouts were labeled with unique $10\text{cm} \times 10\text{cm}$ ArUco markers. Additionally, the topological relations among the markers were recorded and provided as a feed to the framework's *Semantic Perception* database shown in Fig. 2.

Table I presents the collected dataset's characteristics for conducting evaluations. According to the Table, and as shown in Fig. 5, various indoor area setups have been labeled with printed fiducial markers. It should be mentioned that for experiments conducted in the drone testing arena (*i.e.*, *Set-07* and *Set-08*), the installed OptiTrack motion capture system in the laboratory provides ground-truth data. The motion capture system contains twelve high-speed infrared cameras illuminating the reflective markers attached to the

TABLE I: The characteristics of the collected indoor dataset. *Set-07* to *Set-09* were collected in a standard drone-testing arena with accurate ground-truth values provided.

Data	Duration	Description
<i>Set-01</i>	2m 02s	A single room with a door
<i>Set-02</i>	3m 32s	A long corridor with parallel walls and five doors
<i>Set-03</i>	2m 49s	A room within another room (nested)
<i>Set-04</i>	4m 22s	A room with different nested partitions
<i>Set-05</i>	1m 50s	A corridor connected to other rooms and corridors
<i>Set-06</i>	1m 57s	A single room with connected doors
<i>Set-07</i>	2m 06s	AeRoLab Drone-Testing Arena
<i>Set-08</i>	1m 57s	AeRoLab Drone-Testing Arena
Total	20m 35s	



Fig. 5: Some instances of the collected dataset, where ArUco markers are used to label walls and door frames of the environments.

robot that flies within the capture volume. Ground-truth data is provided by identifying and tracking the mounted reflective marker in sequential frames and recording the pose of the flying drone using OptiTrack. However, as it is not possible to record ground-truth data in locations outside the drone-testing arena, other dataset instances are mainly collected to evaluate the performance of the proposed methodology w.r.t. other VSLAM benchmarking frameworks in real-world scenarios.

B. Scene Graphs

Reconstructing the maps of the indoor environments formed by considering geometric and semantic primitives, as well as providing their 3D hierarchical representations enriched with semantic entities, is the primary demand in this paper. This can show the practicality and functionality of the proposed robotics system, which contains a VSLAM software integrated into a drone, and its potential in considering it as an end-to-end application for indoor environment mapping.

Accordingly, Fig. 6 depicts some instances of generated 3D scene graphs using the employed VSLAM framework. The generated hierarchies contain various abstraction levels of semantic entities detected in the environment by the employed system. It should be noted that the correct state of the aerial robot obtained from the visual sensor is required to

perform drift-free state estimation and VSLAM. The figure shows that the walls and door frames are detected and mapped to the global reference frame using the pose of the fiducial markers attached to them. Colored frames and the 3D points with the same color represent the walls and their detected visual features. Detection of rooms (with four walls) and corridors (with two parallel walls), which are shown as cubes, is the next stage handled by the VSLAM. It can be seen that the generated scene graphs give a high-level representation of the environment in which the drone is performing.

C. Experimental Results

Various experiments have been conducted to validate the functionality of the proposed end-to-end system in GPS-denied environments. For evaluating the accuracy of the reconstructed maps, Absolute Pose Error (APE) measurements, including Mean, Root Mean Square Error (RMSE), and Standard Deviation (STD) metrics, are used. Experiments are divided into two main categories described below.

Performance w.r.t. the Ground-truth. In this experiment, dataset instances with provided ground-truth values obtained from the OptiTrack motion capture system are employed. The primary goal of the experiment is to figure out how accurately the proposed VSLAM framework performs for the correct reconstruction of the maps. For this purpose, the data instances were fed to the employed VSLAM framework and ORB-SLAM 3.0 as the baseline, and mean, RMSE, and STD values were calculated.

In this regard, Table II presents the evaluation results of flying the drone in a standard drone-testing arena where the ground-truth is available. According to the table, the employed VSLAM framework works better than its baseline method in both dataset instances. The primary reason for such improvement is applying the poses obtained from fiducial markers and the structural elements (*i.e.*, door frames and walls) to optimize the map. Although the improvement is slight, it can result in an average increase of 6.99% in RMSE and 12.21% in mean measurements. The average STD value of the baseline is better than the employed VSLAM, which can be due to the impact of fiducial markers in estimations. It should be noted that these experimental results are apart from the advantage of the employed VSLAM system in providing 3D scene graphs and hierarchical representation of the environment, which will be discussed in *relative performance evaluations*.

Additionally, Fig. 7 depicts the trajectories generated by the drone experiments, in which the dotted trajectories are ground-truth and the colored ones are estimated. As shown in Table II, the trajectories estimated by the employed framework seem closer to the ground-truth path in some cases.

Relative Performance w.r.t. the Baseline. These experiments are mainly conducted in indoor environments where ground-truth data is unavailable, and the evaluations are obtained by comparing the employed VSLAM methodology w.r.t. ORB-SLAM 3.0. The primary targets of conducting

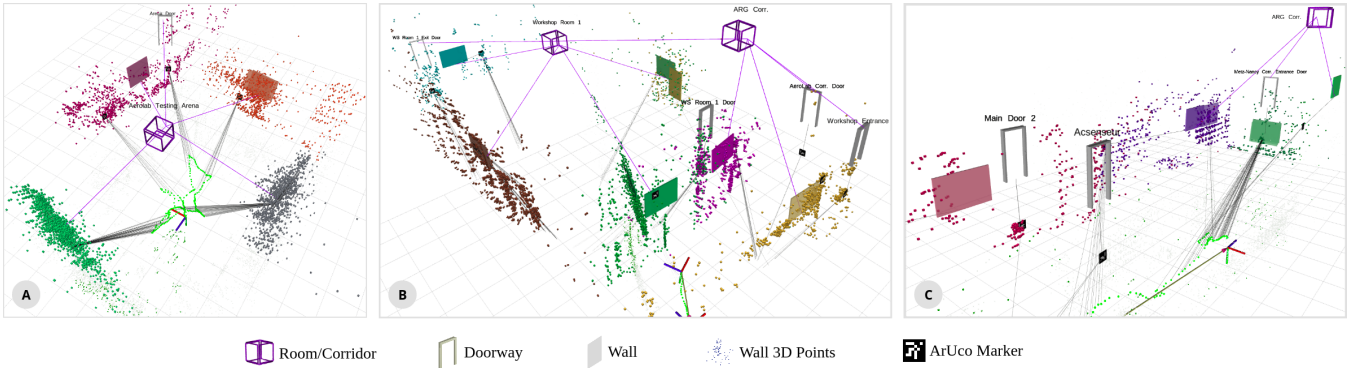


Fig. 6: Some instances of the 3D scene graphs generated by the employed VSLAM framework integrated with a UAV: A) *Set-01*, B) *Set-03*, and C) *Set-05*.

TABLE II: Evaluation results on the collected data instances w.r.t. ground-truth data provided by the OptiTrack motion capture system. The employed metrics are Mean, Root Mean Square Error (RMSE) error in *meters*, and Standard Deviation (STD). The best results are boldfaced.

	Ours [8]			ORB-SLAM 3.0 [33]		
	<i>Mean</i>	<i>RMSE</i>	<i>STD</i>	<i>Mean</i>	<i>RMSE</i>	<i>STD</i>
<i>Set-07</i>	0.2267	0.2689	0.1447	0.251	0.2757	0.1141
<i>Set-08</i>	0.2041	0.2301	0.1027	0.2401	0.2617	0.1042
Overall	0.2158	0.2502	0.1245	0.2458	0.269	0.1093
Improved	12.21%	6.99%	-12.21%	-	-	-

TABLE III: Relative performance evaluation results using the proposed VSLAM system w.r.t. the ORB-SLAM 3.0 on the collected data instances. The metrics used are Maximum, Minimum, Mean, Root Mean Square Error (RMSE) error in *meters*, Sum of Squared Errors (SSE), and Standard Deviation (STD).

	<i>Max.</i>	<i>Mean</i>	<i>Min.</i>	<i>RMSE</i>	<i>SSE</i>	<i>STD</i>
<i>Set-01</i>	0.5276	0.0979	0.0363	0.1108	44.6885	0.0519
<i>Set-02</i>	0.8105	0.0905	0.0239	0.1278	90.9611	0.0903
<i>Set-03</i>	0.9467	0.3403	0.0404	0.3802	623.3242	0.1694
<i>Set-04</i>	4.3524	0.5118	0.0162	0.9652	336.5995	0.8183
<i>Set-05</i>	0.6525	0.0420	0.0028	0.0856	22.191	0.0746
<i>Set-06</i>	0.8738	0.0745	0.0033	0.1261	52.2667	0.1017
Total	1.3606	0.1928	0.0205	0.2993	195.005	0.2177

such experiments are to provide a qualitative assessment of the system, analyze the impact of modifications and adding arbitrary features and semantic entities on the generated outputs, and seek differences in the generated maps. Table III presents the evaluation results of employing the proposed VSLAM system w.r.t. the baseline it has been built upon.

According to the table, the average RMSE and STD values in the comparative analysis are close. It means that the impact of modification and adding different modules to the baseline to identify and map semantic objects still guarantees the quality of the results generated by ORB-SLAM 3.0 as a reliable baseline framework. In other words, the results

are reliable apart from making the drone more situationally aware of the environment by optimizing the generated 3D scene graphs. In scenarios like *Set-04*, where there is a nested room inside another, the RMSE value has the highest value in the table. This can be due to the impact of adding the poses of the structural elements to optimize the map. The situation is reversed in less complicated scenarios, such as *Set-01* and *Set-05*.

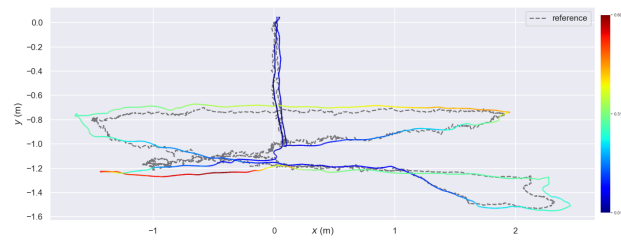
D. Discussions

Considering the experimental results presented above, the proposed VSLAM framework for indoor SLAM map reconstruction and scene graph generation can bring pros and cons. As for the advantages, detecting fiducial markers as helpful components for scene understanding is real-time and does not impose high computational costs on the system. This contrasts with the approaches that require deep learning-based perception and scene processing to detect semantic objects. Moreover, all the processes related to SLAM, structural-level object detection, and fiducial marker recognition are handled in the companion computer used in the drone.

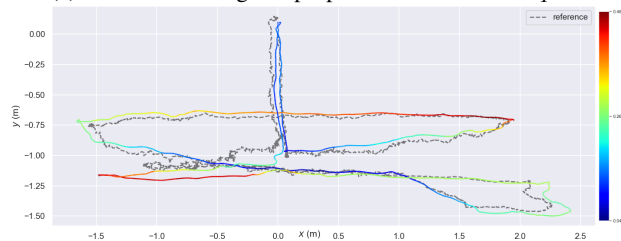
On the other hand, depending on fiducial markers for situational awareness needs to be carefully considered. The fiducial markers might be unreachable, damaged, or obscured in the environment, or maybe even hard to detect because of the blurry images captured due to the shakes caused by the drone while flying. In this regard, missing a fiducial marker may lead to the misdetection of a wall or a door frame in the first step and rooms and corridors afterward. Additionally, any noisy marker detection due to occlusion, poor lighting conditions, etc. can imply wrong pose information in the reconstructed maps. As shown in Table II and Table III, the Standard Deviation value of employing the proposed VSLAM framework can vary a lot. High STD values may indicate the impact of uncertainty and variability in the estimates obtained by the method, which is not desirable in SLAM applications.

V. CONCLUSIONS

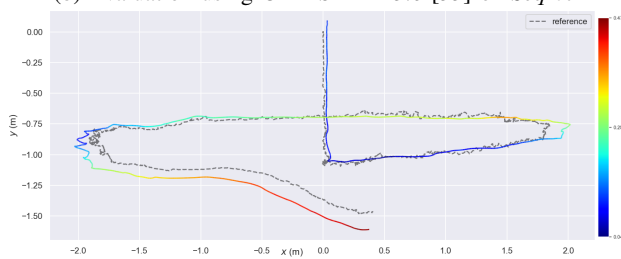
This paper presented an end-to-end system with an integrated Visual SLAM framework into a Unmanned Aerial



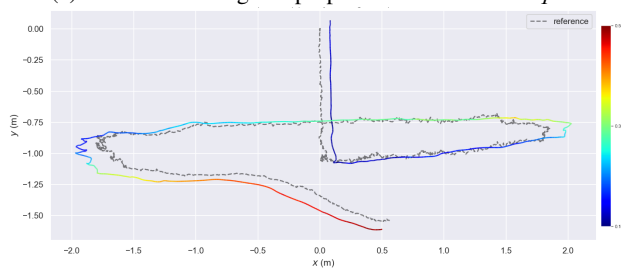
(a) Evaluation using the proposed VSLAM on *Seq-07*



(b) Evaluation using ORB-SLAM 3.0 [33] on *Seq-07*



(c) Evaluation using the proposed VSLAM on *Seq-08*



(d) Evaluation using ORB-SLAM 3.0 [33] on *Seq-08*

Fig. 7: Trajectories traversed using the proposed system in the drone-testing arena. The dotted lines show the ground-truth values fetched by the OptiTrack motion capture system.

Vehicle (UAV) equipped with an RGB-D visual sensor. In this regard, the paper’s primary contribution is introducing a practical solution for utilizing a drone to reconstruct the maps of indoor environments (where GPS measures are not available) alongside generating 3D scene graphs for a high-level representation of the area. The system targets enhancing the situational awareness of the robot while reconstructing maps by incorporating fiducial markers as versatile visual features augmented into structural-semantic elements, including walls and door frames. Detection of higher-semantic entities in the environment, including rooms and corridors, takes place with the aid of the mentioned elements. Various real-world scenario experiments were conducted in indoor areas with dissimilar structural layouts to showcase the proposed system’s practicality. Experimental results showed the proposed

application can reliably provide abstract representations of the maps w.r.t. the ground-truth data.

In future works, equipping the drone with the required modules to perform autonomously is the first step to consider for having an efficient end-to-end system. Additionally, due to the detailed and information-rich maps generated by the introduced system, the authors also plan to utilize it for ”localization and navigation” and ”path planning” in indoor environments. Since the topological information derived from the environment using the VSLAM system is reliable, the current system is expected to properly integrate with the mentioned applications to facilitate decision-making while maintaining the robot’s situational awareness.

REFERENCES

- [1] B. Mishra, D. Garg, P. Narang, and V. Mishra, ”Drone-surveillance for search and rescue in natural disaster,” *Computer Communications*, vol. 156, pp. 1–10, 2020.
- [2] N. Dilshad, J. Hwang, J. Song, and N. Sung, ”Applications and challenges in video surveillance via drone: A brief survey,” in *2020 International Conference on Information and Communication Technology Convergence (ICTC)*. IEEE, 2020, pp. 728–732.
- [3] S. Park, S. Yun, H. Kim, R. Kwon, and J. Ganser, ”Forestry monitoring system using lora and drone,” in *Proceedings of the 8th International Conference on Web Intelligence, Mining and Semantics*, 2018, pp. 1–8.
- [4] R. Krajewski, T. Moers, J. Bock, L. Vater, and L. Eckstein, ”The round dataset: A drone dataset of road user trajectories at roundabouts in germany,” in *2020 IEEE 23rd International Conference on Intelligent Transportation Systems (ITSC)*. IEEE, 2020, pp. 1–6.
- [5] J. Vanhie-Van Gerwen, K. Geebelen, J. Wan, W. Joseph, J. Hoebeke, and E. De Poorter, ”Indoor drone positioning: Accuracy and cost trade-off for sensor fusion,” *IEEE Transactions on Vehicular Technology*, vol. 71, no. 1, pp. 961–974, 2021.
- [6] Y. Akbari, N. Almaadeed, S. Al-Maadeed, and O. Elharrouss, ”Applications, databases and open computer vision research from drone videos and images: a survey,” *Artificial Intelligence Review*, vol. 54, pp. 3887–3938, 2021.
- [7] H. Bavle, J. L. Sanchez-Lopez, C. Cimarelli, A. Tourani, and H. Voos, ”From slam to situational awareness: Challenges and survey,” *Sensors*, vol. 23, no. 10, p. 4849, 2023.
- [8] A. Tourani, H. Bavle, J. L. Sanchez-Lopez, D. I. Avsar, R. M. Salinas, and H. Voos, ”Vision-based situational graphs generating optimizable 3d scene representations,” *arXiv preprint arXiv:2309.10461*, 2023.
- [9] I. Armeni, Z.-Y. He, J. Gwak, A. R. Zamir, M. Fischer, J. Malik, and S. Savarese, ”3d scene graph: A structure for unified semantics, 3d space, and camera,” in *Proceedings of the IEEE International Conference on Computer Vision*, 2019, pp. 5664–5673.
- [10] N. Hughes, Y. Chang, and L. Carlone, ”Hydra: A real-time spatial perception system for 3d scene graph construction and optimization,” 2022.
- [11] H. Bavle, J. L. Sanchez-Lopez, M. Shaheer, J. Civera, and H. Voos, ”Situational graphs for robot navigation in structured indoor environments,” *IEEE Robotics and Automation Letters*, vol. 7, no. 4, pp. 9107–9114, 2022.
- [12] —, ”S-graphs+: Real-time localization and mapping leveraging hierarchical representations,” *IEEE Robotics and Automation Letters*, vol. 8, no. 8, pp. 4927–4934, 2023.
- [13] X. Gao and T. Zhang, *Introduction to visual SLAM: from theory to practice*. Springer Nature, 2021.
- [14] H. Bavle, P. De La Puente, J. P. How, and P. Campoy, ”Vps-slam: Visual planar semantic slam for aerial robotic systems,” *IEEE Access*, vol. 8, pp. 60 704–60 718, 2020.
- [15] M. Kalaitzakis, B. Cain, S. Carroll, A. Ambrosi, C. Whitehead, and N. Vitzilaios, ”Fiducial markers for pose estimation: Overview, applications and experimental comparison of the artag, apriltag, aruco and stag markers,” *Journal of Intelligent & Robotic Systems*, vol. 101, pp. 1–26, 2021.

- [16] S. Garrido-Jurado, R. Muñoz-Salinas, F. J. Madrid-Cuevas, and M. J. Marín-Jiménez, "Automatic generation and detection of highly reliable fiducial markers under occlusion," *Pattern Recognition*, vol. 47, no. 6, pp. 2280–2292, 2014.
- [17] E. Olson, "Apriltag: A robust and flexible visual fiducial system," in *2011 IEEE International Conference on Robotics and Automation*. IEEE, 2011, pp. 3400–3407.
- [18] R. Muñoz-Salinas and R. Medina-Carnicer, "Ucoslam: Simultaneous localization and mapping by fusion of keypoints and squared planar markers," *Pattern Recognition*, vol. 101, p. 107193, 2020.
- [19] F. J. Romero-Ramirez, R. Muñoz-Salinas, M. J. Marín-Jiménez, M. Cazorla, and R. Medina-Carnicer, "sslam: Speeded-up visual slam mixing artificial markers and temporary keypoints," *Sensors*, vol. 23, no. 4, p. 2210, 2023.
- [20] B. Pfrommer and K. Daniilidis, "Tagslam: Robust slam with fiducial markers," 2019. [Online]. Available: <https://arxiv.org/abs/1910.00679>
- [21] G. Raja, S. Suresh, S. Anbalagan, A. Ganapathisubramanian, and N. Kumar, "Pfin: An efficient particle filter-based indoor navigation framework for uavs," *IEEE Transactions on Vehicular Technology*, vol. 70, no. 5, pp. 4984–4992, 2021.
- [22] W. Budiharto, E. Irwansyah, J. S. Suroso, A. Chowanda, H. Ngarianto, and A. A. S. Gunawan, "Mapping and 3d modeling using quadrotor drone and gis software," *Journal of Big Data*, vol. 8, pp. 1–12, 2021.
- [23] S. Bhatnagar, L. Gill, and B. Ghosh, "Drone image segmentation using machine and deep learning for mapping raised bog vegetation communities," *Remote Sensing*, vol. 12, no. 16, p. 2602, 2020.
- [24] Y. Sun, W. Wang, L. Mottola, J. Zhang, R. Wang, and Y. He, "Indoor drone localization and tracking based on acoustic inertial measurement," *IEEE Transactions on Mobile Computing*, 2023.
- [25] A. Famili, A. Stavrou, H. Wang, and J.-M. J. Park, "Pilot: High-precision indoor localization for autonomous drones," *IEEE Transactions on Vehicular Technology*, 2022.
- [26] A. Famili and J.-M. J. Park, "Rolatin: Robust localization and tracking for indoor navigation of drones," in *2020 IEEE Wireless Communications and Networking Conference (WCNC)*. IEEE, 2020, pp. 1–6.
- [27] I. Armeni, Z.-Y. He, J. Gwak, A. R. Zamir, M. Fischer, J. Malik, and S. Savarese, "3d scene graph: A structure for unified semantics, 3d space, and camera," in *Proceedings of the IEEE International Conference on Computer Vision*, 2019, pp. 5664–5673.
- [28] A. Rosinol, A. Gupta, M. Abate, J. Shi, and L. Carlone, "3d dynamic scene graphs: Actionable spatial perception with places, objects, and humans," 2020.
- [29] S.-C. Wu, J. Wald, K. Tateno, N. Navab, and F. Tombari, "Scenegrph-fusion: Incremental 3d scene graph prediction from rgb-d sequences," 2021.
- [30] A. Tourani, H. Bavle, J. L. Sanchez-Lopez, and H. Voos, "Visual slam: What are the current trends and what to expect?" *Sensors*, vol. 22, no. 23, p. 9297, 2022.
- [31] R. Mur-Artal, J. M. M. Montiel, and J. D. Tardos, "Orb-slam: a versatile and accurate monocular slam system," *IEEE transactions on robotics*, vol. 31, no. 5, pp. 1147–1163, 2015.
- [32] R. Mur-Artal and J. D. Tardós, "Orb-slam2: An open-source slam system for monocular, stereo, and rgb-d cameras," *IEEE transactions on robotics*, vol. 33, no. 5, pp. 1255–1262, 2017.
- [33] C. Campos, R. Elvira, J. J. G. Rodríguez, J. M. Montiel, and J. D. Tardós, "Orb-slam3: An accurate open-source library for visual, visual-inertial, and multimap slam," *IEEE Transactions on Robotics*, vol. 37, no. 6, pp. 1874–1890, 2021.
- [34] Y. Fan, Q. Zhang, Y. Tang, S. Liu, and H. Han, "Blitz-slam: A semantic slam in dynamic environments," *Pattern Recognition*, vol. 121, p. 108225, 2022.
- [35] Z. Qian, K. Patath, J. Fu, and J. Xiao, "Semantic slam with autonomous object-level data association," in *2021 IEEE International Conference on Robotics and Automation (ICRA)*. IEEE, 2021, pp. 11 203–11 209.
- [36] K. Doherty, D. Baxter, E. Schneeweiss, and J. Leonard, "Probabilistic data association via mixture models for robust semantic slam," 2019.
- [37] Y. Sun, J. Hu, J. Yun, Y. Liu, D. Bai, X. Liu, G. Zhao, G. Jiang, J. Kong, and B. Chen, "Multi-objective location and mapping based on deep learning and visual slam," *Sensors*, vol. 22, no. 19, p. 7576, 2022.
- [38] P. Guan, Z. Cao, E. Chen, S. Liang, M. Tan, and J. Yu, "A real-time semantic visual slam approach with points and objects," *International Journal of Advanced Robotic Systems*, vol. 17, no. 1, p. 1729881420905443, 2020.
- [39] C. Yu, Z. Liu, X.-J. Liu, F. Xie, Y. Yang, Q. Wei, and Q. Fei, "Dslam: A semantic visual slam towards dynamic environments," in *2018 IEEE/RSJ International Conference on Intelligent Robots and Systems (IROS)*. IEEE, 2018, pp. 1168–1174.
- [40] S. Yang, C. Zhao, Z. Wu, Y. Wang, G. Wang, and D. Li, "Visual slam based on semantic segmentation and geometric constraints for dynamic indoor environments," *IEEE Access*, vol. 10, pp. 69 636–69 649, 2022.
- [41] A. Tourani, H. Bavle, J. L. Sanchez-Lopez, R. M. Salinas, and H. Voos, "Marker-based visual slam leveraging hierarchical representations," in *2023 IEEE/RSJ International Conference on Intelligent Robots and Systems (IROS)*, 2023, pp. 3461–3467.